

EXPLICIT AND IMPLICIT ERROR INHIBITING SCHEMES WITH POST-PROCESSING

ADI DITKOWSKI*, SIGAL GOTTLIEB†, AND ZACHARY J. GRANT‡

Abstract. Efficient high order numerical methods for evolving the solution of an ordinary differential equation are widely used. The popular Runge–Kutta methods, linear multi-step methods, and more broadly general linear methods, all have a global error that is completely determined by analysis of the local truncation error. In prior work in we investigated the interplay between the local truncation error and the global error to construct *error inhibiting schemes* that control the accumulation of the local truncation error over time, resulting in a global error that is one order higher than expected from the local truncation error. In this work we extend our error inhibiting framework introduced in [6] to include a broader class of time-discretization methods that allows an exact computation of the leading error term, which can then be post-processed to obtain a solution that is two orders higher than expected from truncation error analysis. We define sufficient conditions that result in a desired form of the error and describe the construction of the post-processor. A number of new explicit and implicit methods that have this property are given and tested on a variety of ordinary and partial differential equation. We show that these methods provide a solution that is two orders higher than expected from truncation error analysis alone.

1. Introduction. Efficient high order time evolution methods are of interest in many simulations, particularly when evolving in time a system of ordinary differential equations (ODEs) resulting from a semi-discretized partial differential equation. In this work we consider an approach to developing methods that are of higher order than expected from a truncation error analysis. We first present some background on numerical methods for ODEs and define all the relevant terms.

We consider numerical solvers for ordinary differential equations (ODEs) of the form

$$(1) \quad \begin{aligned} u_t &= F(t, u), \quad t \geq 0 \\ u(t^0) &= u_0. \end{aligned}$$

The most basic of these numerical solvers is the forward Euler method

$$v_{n+1} = v_n + \Delta t F(t_n, v_n).$$

Where v_n approximates the exact solution $v_n \approx u(t_n)$ at some time $t^n = t^0 + n\Delta t$. (We typically choose $t^0 = 0$). The forward Euler method has local truncation error LTE^n and approximation error τ^n at any given time t_n defined by

$$\tau^n = \Delta t LTE^n = u(t_{n-1}) + \Delta t F(t_{n-1}, u(t_{n-1})) - u(t_n) \approx O(\Delta t^2)$$

and a global error which is first order accurate

$$E_n = v_n - u(t_n) \approx O(\Delta t).$$

If we want a more accurate method than forward Euler, we can add steps and define a linear multistep method [4]

$$(2) \quad v_{n+1} = \sum_{j=1}^s a_j v_{n+1-j} + \Delta t \sum_{j=0}^s b_j F(t_{n+1-j}, v_{n+1-j}),$$

*School of Mathematical Sciences, Tel Aviv University, Tel Aviv 69978, Israel. Email: adid@post.tau.ac.il

†Mathematics Department, University of Massachusetts Dartmouth, 285 Old Westport Road, North Dartmouth MA 02747. Email: sgottlieb@umassd.edu

‡Department of Computational and Applied Mathematics, Oak Ridge National Laboratory, Oak Ridge TN 37830. Email: grantzj@ornl.gov

or we can use multiple stages as in a Runge–Kutta methods [4]:

$$y_i = v_n + \Delta t \sum_{j=1}^m a_{ij} F(t_n + c_j \Delta t, y_j) \quad \text{for } j = 1, \dots, m$$

$$v_{n+1} = v_n + \Delta t \sum_{j=1}^m b_j F(t_n + c_j \Delta t, y_j).$$

It is also possible to combine the approaches above, as in the general linear methods described in [3, 13]

$$(3) \quad \begin{aligned} y_i &= \sum_{j=1}^s \tilde{U}_{ij} v_j^n + \Delta t \sum_{j=1}^m \tilde{A}_{ij} F(t_n + c_j \Delta t, y_j) \\ v_i^{n+1} &= \sum_{j=1}^s \tilde{V}_{ij} v_j^n + \Delta t \sum_{j=1}^m \tilde{B}_{ij} F(t_n + c_j \Delta t, y_j). \end{aligned}$$

which combines the use of multiple steps and stages. In all these cases, we aim to increase the order of the local truncation error and therefore to increase the order of the global error.

The relationship between the local truncation error and the global error is well-known. The Lax-Richtmeyer equivalence theorem states that if the numerical scheme is stable then the global error is *at least* of the same order as the local truncation error [17, 9, 18]. Indeed, all the familiar schemes for numerically solving ordinary differential equations (ODEs) have global errors that are of the same order as their local truncation errors. In fact, this relationship between local truncation error and global error is common not only for ODE solvers, but is typically seen in other fields in numerical mathematics, such as for finite difference schemes for partial differential equations (PDEs) [9, 18].

It is, however, possible to devise schemes that have global errors that are *higher order* than the local truncation errors. In particular, it was shown in [5] that finite difference schemes for PDEs can be constructed such that their convergence rates are higher than the order of the truncation errors. A similar approach was adopted in [6] for time evolution methods, where we described the conditions under which general linear methods (GLMs) can have global error is *one order higher* than the local truncation error, and devise a number of GLM schemes that feature this behavior. These schemes achieve this higher-than-expected order by inhibiting the lowest order term in the local error from accumulating over time, and so we named them *Error Inhibiting Schemes* (EIS). As we have since discovered, our EIS schemes have the same conditions as the quasi-consistent schemes of Kulikov, Weiner, and colleagues [14, 21, 23].

In this paper, we extend the error inhibiting approach in two ways. First, we consider a broader formulation of the GLM that allows for implicit methods as well as more general explicit methods than considered in [6]. Next, we show that by imposing additional conditions on the methods we are able to precisely describe the coefficients of the error term and we then devise a post-processing approach that removes this error term, thus obtaining a global error that is *two orders higher* than the local truncation error. We proceed to devise error inhibiting methods using this new EIS approach, and investigate their linear stability properties, strong stability preserving (SSP) properties, and computational efficiency. Finally, we test these methods on a

number of numerical examples to demonstrate their enhanced accuracy and, where appropriate, stability properties. In the appendix we present an alternative approach to understanding the growth of the errors and describing the coefficients of the error term.

1.1. Preliminaries. We begin with a scheme of the form

$$(4) \quad V^{n+1} = \mathbf{D}V^n + \Delta t \mathbf{A}F(V^n) + \Delta t \mathbf{R}F(V^{n+1}),$$

where V^n is a vector of length s that contains the numerical solution at times $(t_n + c_j \Delta t)$ for $j = 1, \dots, s$:

$$(5) \quad V^n = (v(t_n + c_1 \Delta t), v(t_n + c_2 \Delta t), \dots, v(t_n + c_s \Delta t))^T.$$

The function $F(V^n)$ is defined as the component-wise function evaluation on the vector V^n :

$$(6) \quad F(V^n) = (F(v(t_n + c_1 \Delta t)), F(v(t_n + c_2 \Delta t)), \dots, F(v(t_n + c_s \Delta t)))^T.$$

For convenience, $c_1 \leq c_2 \leq \dots \leq c_s$. Also, we pick $c_s = 0$ so that the final element in the vector approximates the solution at time t_n . This notation was chosen to match the notation widely used in the field of general linear methods. To start these methods, we need to build an initial vector: to do so we artificially redefine the time-grid so that $t_0 = t^0 - c_1 \Delta t$. Now the first element in the initial solution vector V^0 is $v(t_0 + c_1 \Delta t) = u(t^0)$ and the remaining elements $v(t_0 + c_j \Delta t)$ are computed using a highly accurate one-step method.

REMARK 1. *The form (4) includes implicit schemes, as V^{n+1} appears on both sides of the equation. However, if \mathbf{R} is strictly lower triangular the scheme is, in fact, explicit. If \mathbf{R} is a diagonal matrix then we can compute each element of the vector V^{n+1} concurrently.*

We define the corresponding exact solution of the ODE (1):

$$(7) \quad U^n = (u(t_n + c_1 \Delta t), u(t_n + c_2 \Delta t), \dots, u(t_n + c_s \Delta t))^T,$$

with $F(U^n)$ defined similarly.

The *global error* of the method is defined as the difference between the vectors of the exact and the numerical solutions at some time t^n

$$(8) \quad E^n = V^n - U^n.$$

The method (4) has a local truncation error LTE^n and approximation error $\boldsymbol{\tau}^n$, where these vector are defined by

$$(9) \quad \Delta t LTE^n = \boldsymbol{\tau}^n = [\mathbf{D}U^{n-1} + \Delta t \mathbf{A}F(U^{n-1}) + \Delta t \mathbf{R}F(U^n)] - U^n$$

where

$$(10) \quad \boldsymbol{\tau}^n = \sum_{j=0}^{\infty} \boldsymbol{\tau}_j^n \Delta t^j = \sum_{j=0}^{\infty} \boldsymbol{\tau}_j \Delta t^j \left. \frac{d^j u}{dt^j} \right|_{t=t_n}$$

and

$$(11a) \quad \boldsymbol{\tau}_0 = (\mathbf{I} - \mathbf{D}) \mathbf{1}$$

$$(11b) \quad \boldsymbol{\tau}_j = \frac{1}{(j-1)!} \left(\frac{1}{j} \mathbf{D}(\mathbf{c} - \mathbf{1})^j + \mathbf{A}(\mathbf{c} - \mathbf{1})^{j-1} + \mathbf{R}\mathbf{c}^{j-1} - \frac{1}{j} \mathbf{c}^j \right)$$

for $j=1, 2, \dots$

Here, \mathbf{c} is the vector of abscissas $(c_1, c_2, \dots, c_s)^T$ and $\mathbf{1} = (1, 1, \dots, 1)^T$ is the vector of ones. Terms of the form \mathbf{c}^j are understood component-wise $\mathbf{c}^j = (c_1^j, c_2^j, \dots, c_s^j)^T$.

A scheme with local truncation error $LTE^n = O(\Delta t^p)$ and (correspondingly) approximation error $\tau^n = O(\Delta t^{p+1})$ has $\tau_j = 0$ for $j = 0, \dots, p$. In such a case we typically observe a global order of $E^n = O(\Delta t^p)$ at any time t^n . As shown in [6], if we add conditions on \mathbf{D} , \mathbf{A} (and \mathbf{R}), we can find methods that exhibit a global order of $E^n = O(\Delta t^{p+1})$ even though they only satisfy $\tau_j = 0$ for $j = 0, \dots, p$. In addition, as we show in Section 3.2, certain conditions on \mathbf{D} , \mathbf{A} , \mathbf{R} allow us to precisely understand the form of the Δt^{p+1} term in the global error, so we can design a postprocessor that gives us a numerical solution which has an error of order $O(\Delta t^{p+2})$, as we show in Section 3.3.

2. Review of error inhibiting and related schemes. The celebrated Lax-Richtmeyer equivalence theorem (see e.g. [17], [9], [18]) states that if the numerical scheme is stable then the global error is *at least* of the same order as the local truncation error. All the one step methods and linear multi-step methods that are commonly used feature a global error that is of the same order as the normalized local truncation error. This is so common that the order of the method is typically defined solely by the order conditions derived by Taylor series analysis of the local truncation error. However, recent work [6] has shown that one can construct general linear methods so that the accumulation of the local truncation error over time is controlled. These schemes feature a global error that is one order higher than the local truncation error. In this section we review prior work on such error inhibiting schemes by Ditkowski and Gottlieb [6], and show that similar results were obtained in the work of Kulikov, Weiner, and colleagues [14, 21, 23]. This body of work serves as the basis for our current work which will be presented in Section 3.

In [6], Gottlieb and Ditkowski showed that given a numerical method of the form

$$(12) \quad V^{n+1} = \mathbf{D}V^n + \Delta t \mathbf{A}F(V^n)$$

(i.e. 4 with $\mathbf{R} = 0$), where \mathbf{D} is a diagonalizable rank one matrix, whose non-zero eigenvalue is equal to one and its corresponding eigenvector is $(1, \dots, 1)^T$, if the method satisfies the order conditions

$$(13) \quad \tau_j = 0, \quad \text{for } j = 0, \dots, p$$

and the *error inhibiting condition*

$$(14) \quad \mathbf{D}\tau_{p+1} = 0$$

hold, then the resulting global error satisfies $E^n = O(\Delta t^{p+1})$. That work [6] showed how condition (14) mitigates the accumulation of the truncation error, so we obtain a global error that is one order *higher* than predicted by the order conditions that describe the local truncation error. Furthermore, the authors developed several block one-step methods and demonstrated in numerical examples on nonlinear problems (including a nonlinear system) that these methods have global error that is one order higher than the local truncation error analysis predicts.

As we later found out, although the underlying approach is different, the conditions in [6] are along the theory of quasi-consistency first introduced by Skeel in 1978 [19]. This work was then generalized and further developed by Kulikov for Nordsieck methods in [14], as well as Weiner and colleagues [23]. In [23], a theory of superconvergence for explicit two-step peer methods was defined. In these papers, the authors

showed that if the method satisfies order conditions (13) and conditions that are equivalent to the EIS conditions in [6] then the global error satisfies $E^n = O(\Delta t^{p+1})$. A similar theory was developed for implicit-explicit methods in [21].

In [15], [22], and [16], the authors show that by requiring the order conditions (13) and EIS condition (14) as well as additional conditions

$$(15a) \quad \mathbf{D}\boldsymbol{\tau}_{p+2} = 0$$

$$(15b) \quad \mathbf{D}\mathbf{A}\boldsymbol{\tau}_{p+1} = 0$$

$$(15c) \quad \mathbf{D}\mathbf{R}\boldsymbol{\tau}_{p+1} = 0$$

the resulting global error satisfies $E^n = O(\Delta t^{p+1})$ but, in addition, the form of the first surviving term in the global error (the vector multiplying Δt^{p+1}) is known explicitly, and is leveraged for error estimation.

In fact, we can show that under less restrictive conditions than (15) we can explicitly compute the form of the first surviving term in the global error. Furthermore, having this error term explicitly defined allows us to define a postprocessor that allows us to extract a final-time solution that is accurate to two orders higher than predicted by truncation error analysis alone. We proceed to demonstrate these two facts and design a post-processor that allows us to extract a solution of $O(\Delta t^{p+2})$.

3. Designing explicit and implicit error inhibiting schemes with post-processing. In this section we consider the improved error inhibiting schemes and the associated post-processor that allow us to recover order $p + 2$ from a scheme that would otherwise be only p th order accurate. In Subsection 3.2, we show that the method must satisfy additional conditions so that the form of the final error is controlled and can be post-processed to extract higher order. In Subsection 3.3, we show how this post-processing is done. Before we begin, we make some observations in Subsection 3.1 that will be essential for Subsection 3.2.

3.1. Essentials. In this subsection we present two observations that will be used in the next subsection. The first observation uses the smoothness of the time evolution operator to bound the growth of the error at each step:

LEMMA 1. *The scheme (4) can be written in the form:*

$$(16) \quad V^{n+1} = (I - \Delta t \mathbf{R}F)^{-1} (\mathbf{D} + \Delta t \mathbf{A}F) V^n \equiv Q^n V^n$$

If the order conditions are satisfied to $j = 0, \dots, p$, the scheme (4) (or equivalently (16)) is zero-stable, the operator $(I - \Delta t \mathbf{R}F)^{-1}$ is bounded and the (nonlinear) operator Q^n is Lipschitz continuous in the sense that there is some constant $L > 0$ such that

$$(17) \quad \|Q^n V^n - Q^n U^n\| \leq L \|V^n - U^n\|$$

then the error accumulated in one step gets no worse than $O(\Delta t^{p+1})$ i.e.

$$(18) \quad \|E^{n+1}\| = O(\|E^k\|) + O(\Delta t^{p+1}).$$

Proof. The exact solution satisfies the equation

$$(19) \quad U^{n+1} = Q^n U^n - (I - \Delta t \mathbf{R}F)^{-1} \boldsymbol{\tau}^{n+1}.$$

By subtracting (19) from (16) we obtain

$$\begin{aligned}\|E^{n+1}\| &= \|V^{n+1} - U^{n+1}\| \leq \|Q^n V^n - Q^n U^n\| + \|(I - \Delta t \mathbf{R} F)^{-1} \tau^{n+1}\| \\ &\leq L \|V^n - U^n\| + O(\Delta t^{p+1}) \\ &= O(\|E^k\|) + O(\Delta t^{p+1}).\end{aligned}\quad \square$$

The next observation will be needed for the expansion of $F(U^n + E^n)$:

LEMMA 2. *Given a smooth enough function F , we have*

$$(20) \quad F(U^n + E^n) = F(U^n) + F_y^n E^n + O(\Delta t)O(\|E^n\|),$$

where $F_y^n = F_y(u(t_n))$.

Proof. We expand

$$F(U^n + E^n) = F(U^n) + \begin{pmatrix} F_y(u(t_n + c_1 \Delta t))e_{n+c_1} \\ F_y(u(t_n + c_2 \Delta t))e_{n+c_2} \\ \vdots \\ F_y(u(t_n + c_s \Delta t))e_{n+c_s} \end{pmatrix} + O(\|E^n\|^2),$$

where the error vector is $E^n = (e_{n+c_1}, e_{n+c_2}, \dots, e_{n+c_s})^T$.

Using the definition $F_y^{n+c_j} = F_y(u(t_n + c_j \Delta t))$ we re-write this as

$$F(U^n + E^n) = F(U^n) + \begin{pmatrix} F_y^{n+c_1} & 0 & \dots & 0 \\ 0 & F_y^{n+c_2} & \dots & 0 \\ \vdots & \vdots & \ddots & \vdots \\ 0 & 0 & \dots & F_y^{n+c_s} \end{pmatrix} E^n + O(\|E^n\|^2).$$

Each term can be expanded as

$$F_y^{n+c_j} = F_y(u(t_n + c_j \Delta t)) = F_y(u(t_n)) + c_j \Delta t F_{yy}(u(t_n)) + O(\Delta t^2)$$

so that

$$\begin{aligned}F(U^n + E^n) &= F(U^n) + (F_y^n I + O(\Delta t)) E^n + O(\|E^n\|^2) \\ &= F(U^n) + F_y^n E^n + O(\Delta t)O(\|E^n\|).\end{aligned}\quad \square$$

COROLLARY 1. *If the error is of the form $E^n = O(\Delta t^{p+1})$, then*

$$(21) \quad F(U^n + E^n) = F(U^n) + F_y^n E^n + O(\Delta t^{p+2}).$$

3.2. Improved error inhibiting schemes that have $p + 1$ order. In this section we consider a method of the form (4), where \mathbf{D} is a rank one method that satisfies the consistency condition $\mathbf{D}\mathbf{1} = \mathbf{1}$, and \mathbf{D} , \mathbf{A} and \mathbf{R} are matrices that satisfy the order conditions

$$(22) \quad \tau_j = 0, \quad \text{for } j = 1, \dots, p,$$

and the EIS+ conditions

$$(23a) \quad \mathbf{D}\tau_{p+1} = 0$$

$$(23b) \quad \mathbf{D}\tau_{p+2} = 0$$

$$(23c) \quad \mathbf{D}(\mathbf{A} + \mathbf{R})\tau_{p+1} = 0.$$

We initialize the method with a numerical solution vector V^0 that is accurate enough so that we ensure that the error is negligible. This means that taking one step forward using (4) has no accumulation error, only the truncation error:

$$V^1 = U^1 + \tau^1 = U^1 + \Delta t^{p+1} \boldsymbol{\tau}_{p+1}^1 + \Delta t^{p+2} \boldsymbol{\tau}_{p+2}^1 + O(\Delta t^{p+3}),$$

and

$$E^1 = \Delta t^{p+1} \boldsymbol{\tau}_{p+1}^1 + \Delta t^{p+2} \boldsymbol{\tau}_{p+2}^1 + O(\Delta t^{p+3}).$$

The conditions $\mathbf{D}\boldsymbol{\tau}_{p+1} = 0$ and $\mathbf{D}\boldsymbol{\tau}_{p+2} = 0$ from (23) mean that

$$\mathbf{D}E^1 = O(\Delta t^{p+3}).$$

From Lemma 1 we know that the error that accumulates in only one step is no worse than order Δt^{p+1} so that $O(E^{k+1}) = O(E^k) + O(\Delta t^{p+1})$ and thus we know that

$$V^2 = U^2 + O(\Delta t^{p+1}).$$

We use these facts about V^1 and V^2 to write:

$$\begin{aligned} V^2 &= \mathbf{D}V^1 + \Delta t \mathbf{A}F(V^1) + \Delta t \mathbf{R}F(V^2) \\ &= \mathbf{D}(U^1 + E^1) + \Delta t \mathbf{A}F(U^1 + E^1) + \Delta t \mathbf{R}F(U^2 + E^2) \\ &= \mathbf{D}(U^1 + E^1) + \Delta t \mathbf{A}F(U^1 + E^1) + \Delta t \mathbf{R}F(U^2 + O(\Delta t^{p+1})) \\ &= [\mathbf{D}U^1 + \Delta t \mathbf{A}F(U^1) + \Delta t \mathbf{R}F(U^2)] + \mathbf{D}E^1 + O(\Delta t^{p+2}) \\ &= [\mathbf{D}U^1 + \Delta t \mathbf{A}F(U^1) + \Delta t \mathbf{R}F(U^2)] + O(\Delta t^{p+2}). \end{aligned}$$

Note that the first three terms are, by the definition of the local truncation error

$$\mathbf{D}U^1 + \Delta t \mathbf{A}F(U^1) + \Delta t \mathbf{R}F(U^2) = U^2 + \Delta t^{p+1} \boldsymbol{\tau}_{p+1}^2 + \Delta t^{p+2} \boldsymbol{\tau}_{p+2}^2 + O(\Delta t^{p+3}),$$

so that

$$V^2 = U^2 + \boldsymbol{\tau}^2 + O(\Delta t^{p+2}),$$

which means that

$$E^2 = \boldsymbol{\tau}^2 + O(\Delta t^{p+2}).$$

Using this more refined understanding of the order term, we repeat the process above to write:

$$\begin{aligned} V^2 &= \mathbf{D}(U^1 + E^1) + \Delta t \mathbf{A}F(U^1 + E^1) + \Delta t \mathbf{R}F(U^2 + E^2) \\ &= [\mathbf{D}U^1 + \Delta t \mathbf{A}F(U^1) + \Delta t \mathbf{R}F(U^2)] + \mathbf{D}E^1 + \Delta t \mathbf{A}E^1 F_y^1 + \Delta t \mathbf{R}E^2 F_y^2 + O(\Delta t^{2p+3}) \\ &= U^2 + \boldsymbol{\tau}^2 + \Delta t \mathbf{A}\boldsymbol{\tau}^1 F_y^1 + \Delta t \mathbf{R}\boldsymbol{\tau}^2 F_y^2 + O(\Delta t^{p+3}) \\ &= U^2 + \boldsymbol{\tau}^2 + \Delta t^{p+2} \mathbf{A}\boldsymbol{\tau}_{p+1}^1 F_y^1 + \Delta t^{p+2} \mathbf{R}\boldsymbol{\tau}_{p+1}^2 F_y^2 + O(\Delta t^{p+3}) \\ &= U^2 + \boldsymbol{\tau}^2 + \Delta t^{p+2} (\mathbf{A} + \mathbf{R}) \boldsymbol{\tau}_{p+1}^2 F_y^2 + O(\Delta t^{p+3}) \\ &= U^2 + \Delta t^{p+1} \boldsymbol{\tau}_{p+1}^2 + \Delta t^{p+2} \boldsymbol{\tau}_{p+2}^2 + \Delta t^{p+2} (\mathbf{A} + \mathbf{R}) \boldsymbol{\tau}_{p+1}^2 F_y^2 + O(\Delta t^{p+3}). \end{aligned}$$

This means that

$$(24) \quad E^2 = \Delta t^{p+1} \boldsymbol{\tau}_{p+1}^2 + \Delta t^{p+2} \boldsymbol{\tau}_{p+2}^2 + \Delta t^{p+2} (\mathbf{A} + \mathbf{R}) \boldsymbol{\tau}_{p+1}^2 F_y^2 + O(\Delta t^{p+3}),$$

and so conditions (23) imply that

$$\mathbf{D}E^2 = O(\Delta t^{p+3}).$$

This precise form of E^2 can be extended to the error at any time-level t_n . In the following theorem we show that the conditions (23) allow us to determine the precise form of the Δt^{p+1} term in the global error E^n resulting from the scheme (4). In the next section we use this precise form to extract higher order accuracy by post-processing.

THEOREM 1. *For a method of the form (4), if we choose a rank one matrix \mathbf{D} such that the consistency condition $\mathbf{D}\mathbf{1} = \mathbf{1}$ is satisfied, and matrices \mathbf{A} and \mathbf{R} such that the order conditions (22) are satisfied and furthermore the EIS conditions (23) hold, then the resulting global error at any time t_n has the form*

$$(25) \quad E^n = \Delta t^{p+1} \tau_{p+1}^n + \Delta t^{p+2} \tau_{p+2}^n + \Delta t^{p+2} (\mathbf{A} + \mathbf{R}) \tau_{p+1}^n F_y^n + C_n n \Delta t^{p+3} + O(\Delta t^{p+3}),$$

where C_n is a constant.

Proof. We showed above that the base case (24) has the correct form (25). We proceed by induction: assume that the numerical solution at time t^k has an error of the form (25):

$$E^k = \Delta t^{p+1} \tau_{p+1}^k + \Delta t^{p+2} \tau_{p+2}^k + \Delta t^{p+2} (\mathbf{A} + \mathbf{R}) \tau_{p+1}^k F_y(U^k) + C_k k \Delta t^{p+3} + O(\Delta t^{p+3}).$$

This means that, using conditions (23), we have

$$\mathbf{D}E^k = C_k k \Delta t^{p+3} + O(\Delta t^{p+3}).$$

We wish to show that under the conditions in the theorem, E^{k+1} has a similar form. We split our argument into two steps:

(1) First step: We know from Lemma 1 that the error that accumulates in only one step is no worse than order Δt^{p+1} so that since $E^k = O(\Delta t^{p+1})$ we know that we also have $E^{k+1} = O(\Delta t^{p+1})$. Now we look at the evolution of the error from one time-step to the next:

$$\begin{aligned} V^{k+1} &= \mathbf{D}V^k + \Delta t \mathbf{A}F(V^k) + \Delta t \mathbf{R}F(V^{k+1}) \\ &= \mathbf{D}(U^k + E^k) + \Delta t \mathbf{A}F(U^k + E^k) + \Delta t \mathbf{R}F(U^{k+1} + E^{k+1}) \\ &= [\mathbf{D}U^k + \Delta t \mathbf{A}F(U^k) + \Delta t \mathbf{R}F(U^{k+1})] + \mathbf{D}E^k + O(\Delta t^{p+2}) \\ &= U^{k+1} + \tau^{k+1} + O(\Delta t^{p+2}) \end{aligned}$$

so that

$$E^{k+1} = \Delta t^{p+1} \tau_{p+1}^{k+1} + O(\Delta t^{p+2}).$$

(2) Second step: This analysis allowed us to obtain a more precise understanding of the growth of the error over one step from V^k to V^{k+1} . The error is still of order $O(\Delta t^{p+1})$, but the leading term in the error is now explicitly defined. With this new understanding of V^{k+1} , we repeat the analysis:

$$\begin{aligned} V^{k+1} &= \mathbf{D}V^k + \Delta t \mathbf{A}F(V^k) + \Delta t \mathbf{R}F(V^{k+1}) \\ &= \mathbf{D}(U^k + E^k) + \Delta t \mathbf{A}F(U^k + E^k) + \Delta t \mathbf{R}F(U^{k+1} + E^{k+1}) \\ &= [\mathbf{D}U^k + \Delta t \mathbf{A}F(U^k) + \Delta t \mathbf{R}F(U^{k+1})] + \mathbf{D}E^k \\ &\quad + \Delta t \mathbf{A}E^k F_y^k + \Delta t \mathbf{R}E^{k+1} F_y^{k+1} + O(\Delta t^{2p+3}) \\ &= U^{k+1} + \tau^{k+1} + \Delta t \mathbf{A}E^k F_y^k + \Delta t \mathbf{R}E^{k+1} F_y^{k+1} + C_k k \Delta t^{p+3} + O(\Delta t^{p+3}). \end{aligned}$$

Recall that

$$\boldsymbol{\tau}_{p+1}^{k+1} = \boldsymbol{\tau}_{p+1}^k + O(\Delta t) \quad \text{and} \quad F_y^{k+1} = F_y^k + O(\Delta t),$$

so that

$$\Delta t \mathbf{R} E^{k+1} F_y^{k+1} = \Delta t^{p+2} \mathbf{R} \boldsymbol{\tau}_{p+1}^{k+1} F_y^{k+1} + \frac{1}{2} \tilde{C} \Delta t^{p+3} + O(\Delta t^{p+4}),$$

and

$$\Delta t \mathbf{A} E^k F_y^k = (\Delta t^{p+2} \mathbf{A} \boldsymbol{\tau}_{p+1}^k + O(\Delta t^{p+3})) F_y^k = \Delta t^{p+2} \mathbf{A} \boldsymbol{\tau}_{p+1}^k F_y^{k+1} + \frac{1}{2} \tilde{C} \Delta t^{p+3} + O(\Delta t^{p+4}).$$

Also, we can write

$$\boldsymbol{\tau}^{k+1} = \Delta t^{p+1} \boldsymbol{\tau}_{p+1}^{k+1} + \Delta t^{p+2} \boldsymbol{\tau}_{p+2}^{k+1} + \frac{1}{2} \tilde{C} \Delta t^{p+3} + O(\Delta t^{p+4}).$$

Clearly, each time-step accumulates a few terms of the form Δt^{p+3} . Plugging this back in above gives us

$$\begin{aligned} V^{k+1} &= U^{k+1} + \Delta t^{p+1} \boldsymbol{\tau}_{p+1}^{k+1} + \Delta t^{p+2} \boldsymbol{\tau}_{p+2}^{k+1} + \Delta t^{p+2} (\mathbf{A} + \mathbf{R}) \boldsymbol{\tau}_{p+1}^{k+1} F_y^{k+1} \\ &\quad + (C_k k + \tilde{C}) \Delta t^{p+3} + O(\Delta t^{p+3}) \end{aligned}$$

Setting $C_{k+1} = \max\{C_k, \tilde{C}\}$ we obtain the desired result. \square

The conditions $\boldsymbol{\tau}_j = 0$ for $j = 1, \dots, p$ give us a method of order p , while the additional condition $\mathbf{D} \boldsymbol{\tau}_{p+1}^n = 0$ allow us to get a $p + 1$ order method, just as in previous EIS methods. Adding the conditions $\mathbf{D} \boldsymbol{\tau}_{p+2}^n = 0$ and $\mathbf{D}(\mathbf{A} + \mathbf{R}) \boldsymbol{\tau}_{p+1}^n = 0$ does not give us a higher order scheme. However, it allows us to control the growth of the error so that we can identify the error terms as in (25). This, in turn, allows us to design a postprocessor that extracts order $p + 2$, as we show in the next subsection.

3.3. Post-processing to recover $p + 2$ order. In Theorem 1 we showed that the at every time-step t_n the error E^n has the form (25). The leading order term $\Delta t^{p+1} \boldsymbol{\tau}_{p+1}^n$ can be filtered at the end of the computation in a post-processing stage as long as $\boldsymbol{\tau}_{p+1}^n$ lies in a subspace which is “distinct enough” from the exact solution.

First we note that for the error to be of order Δt^{p+2} the exact solution of the ODE must have at least $p + 2$ smooth derivatives, i.e. $u(t) \in C^{p+2}$. Therefore, up to an error of order $p + 2$, we can expand the solution as a polynomial of degree $p + 1$

$$(26) \quad u(t) = \sum_{j=0}^{p+1} a_j (t - t_\nu)^j + O(\Delta t^{p+2})$$

at any point in the interval $[t_\nu - \Delta t, t_\nu + \Delta t]$. It is then reasonable to expect that the numerical solution, V^n , can be similarly expanded. Our post-processor is built on these observations.

To build the post-processor, we define the time vector to be the temporal grid points in the last two computation steps:

$$(27) \quad \begin{aligned} \tilde{\mathbf{t}} &= (t_{n-1} + c_1 \Delta t, \dots, t_{n-1} + c_s \Delta t, t_n + c_1 \Delta t, \dots, t_n + c_s \Delta t)^T \\ &= \begin{pmatrix} \mathbf{1} t_n + (\mathbf{c} - \mathbf{1}) \Delta t \\ \mathbf{1} t_n + \mathbf{c} \Delta t \end{pmatrix}. \end{aligned}$$

The last term in (27) states that the vectors $\mathbb{1}t_n + (\mathbf{c} - \mathbb{1})\Delta t$ and $\mathbb{1}t_n + \mathbf{c}\Delta t$ are concatenated into one $2s$ long vector. Correspondingly, we let

$$\tilde{V}^n = \begin{pmatrix} V^{n-1} \\ V^n \end{pmatrix} \quad \text{and} \quad \tilde{U}^n = \begin{pmatrix} U^{n-1} \\ U^n \end{pmatrix}$$

i.e., as for the temporal grid, the numerical solutions V^{n-1} and V^n are concatenated into one long vector, and the same is done for the exact solutions U^{n-1} and U^n . Similarly we define a concatenation of the leading truncation error terms

$$(28) \quad \tilde{\boldsymbol{\tau}} = \begin{pmatrix} \boldsymbol{\tau}_{p+1} \\ \boldsymbol{\tau}_{p+1} \end{pmatrix},$$

where $\boldsymbol{\tau}_{p+1}$ was defined in (11). Note that by (25),

$$(29) \quad \tilde{E}^n = \begin{pmatrix} E^{n-1} \\ E^n \end{pmatrix} = \tilde{\boldsymbol{\tau}} \Delta t^{p+1} \left. \frac{d^j u}{dt^j} \right|_{t=t_n} + O(\Delta t^{p+2}).$$

Let $P_0(t - t_n), \dots, P_{p+1}(t - t_n)$ be a set of polynomials of degree less or equal to $p + 1$ such that

$$(30) \quad \text{span} \{P_0(t - t_n), \dots, P_{p+1}(t - t_n)\} = \text{span} \{1, (t - t_n), \dots, (t - t_n)^{p+1}\}$$

and that the vectors $\mathbf{P}_0, \dots, \mathbf{P}_{p+1}$ are the projections of $P_0(t - t_n), \dots, P_{p+1}(t - t_n)$ onto the temporal grid points $\tilde{\mathbf{t}}$.

Define the matrix $T \in \mathbb{C}^{2s \times 2s}$ as follows; The first column is $\tilde{\boldsymbol{\tau}}$, the next $p + 2$ columns are $\mathbf{P}_0, \dots, \mathbf{P}_{p+1}$, and the remaining $2s - (p + 3)$ columns are selected such that T can be inverted. A convenient way to accomplish this is to define the Vandermonde interpolation matrix on the points in the $2s$ -length vector $\tilde{\mathbf{t}}$ and replace the highest order column (in MATLAB the first column) by $\tilde{\boldsymbol{\tau}}$.

The post-processing filter is then given by

$$(31) \quad \Phi = T \text{diag} \left(\underbrace{0, 1, \dots, 1}_{p+2}, \underbrace{*, \dots, *}_{2s-(p+3)} \right) T^{-1}$$

Where we select $*$ to be either 1 or 0, if it is desired to keep this subspace or eliminate it, respectively. Note that, by construction, the matrix Φ multiplied to the error vector \tilde{E}^n eliminates the leading order term

$$(32) \quad \Phi \tilde{E}_n = O(\Delta t^{p+2}).$$

Using the polynomial expansion of \tilde{U}^n assumed in (26) we obtain

$$(33) \quad \Phi \tilde{U}^n = \tilde{U}_n + O(\Delta t^{p+2}),$$

and therefore the numerical solution obtained after the post-processing stage is of order $p + 2$:

$$(34) \quad \Phi \tilde{V}^n = \Phi \left(\tilde{U}^n + \tilde{E}_n \right) = \tilde{U}_n + O(\Delta t^{p+2}).$$

REMARK 2. We note that is important that the leading term of the error does not live in the span of these polynomials. In other words, we need $\tilde{\tau} \notin \text{span}\{\mathbf{P}_0, \dots, \mathbf{P}_{p+1}\}$. It is also important that the leading term of the error does not live too close to the space spanned by these polynomials. The coefficient in the $O(\Delta t^{p+2})$ term of (34) depends on the norm of the matrix Φ . This norm, in turn, is related to how far $\tilde{\tau}$ is from its projection into the subspace $\text{span}\{\mathbf{P}_0, \dots, \mathbf{P}_{s+1}\}$. To avoid numerical instability, it should be verified during the design stage that $\|\Phi\|$ is not “too large”.

Despite the verbose description above, the design of the post-processor matrix is computationally simple. The following MATLAB code shows how the postprocessing matrix P is computed:

```
m = 2; % # of intervals
TAU = repmat(tau(:,p-1),m,1) ; % truncation error vector
gp = c-(m-1:-1:0); % Gridpoints
S = (vander(gp(:))); % Polynomial basis
S(:,1) = TAU; % Put TAU into basis
DD = diag([0,ones(1,length(S)-1)]); % Zero out truncation error
Phi = S*DD*inv(S); % Build post-processing matrix
```

In the preceding discussion we assumed that there are enough points in time in each interval to produce a high enough order polynomial: in other words, we assumed that

$$2s \geq p + 3.$$

When this is not correct (e.g. when we have a scheme with $s = 2$ that has $p = 2$, or a scheme with $s = 3$ that has $p = 4$) we need to use three repeats of each vector so that

$$3s \geq p + 3.$$

In the MATLAB code above this is equivalent to choosing $m = 3$.

4. New error inhibiting schemes with post-processing. Using MATLAB we coded an optimization problem [8] that finds the coefficients $\mathbf{D}, \mathbf{A}, \mathbf{R}$ that satisfy the consistency and order conditions (22) and the error inhibiting conditions (23) while maximizing such properties as the linear stability region or the strong stability preserving coefficient [11]. In this section we present some new methods obtained by the optimization code. These methods are error inhibiting (i.e. they satisfy (23a)) and one order higher can be extracted by postprocessing (i.e. they satisfy (23b) and (23c) as well).

4.1. Explicit Methods. In this section we present the explicit error inhibiting methods that can be post-processed. For each method we present the coefficients $\mathbf{D}, \mathbf{A}, \mathbf{R}$. We also give values of the abscissas and the truncation error vector that must be used to construct the postprocessor. We denote an explicit s -step method that satisfies the conditions (23) and can be postprocessed to order p as eEIS+(s,p). If, in addition, the method is also strong stability preserving, we denote it eSSP-EIS+(s,p).

Explicit error inhibiting method eEIS+(2,4): This explicit two stage error inhibiting method is fourth order if it is post processed, otherwise it gives third order accurate solutions. The coefficients are:

$$D = \frac{1}{2} \begin{pmatrix} 1 & 1 \\ 1 & 1 \end{pmatrix}, \quad A = \frac{1}{12} \begin{pmatrix} -7 & 17 \\ 7 & -5 \end{pmatrix}, \quad R = \begin{pmatrix} 0 & 0 \\ 1 & 0 \end{pmatrix}.$$

The abscissas are $c_1 = -\frac{1}{3}, c_2 = 0$. The truncation error vector is $\boldsymbol{\tau}_3 = \frac{55}{324} (1, -1)^T$.

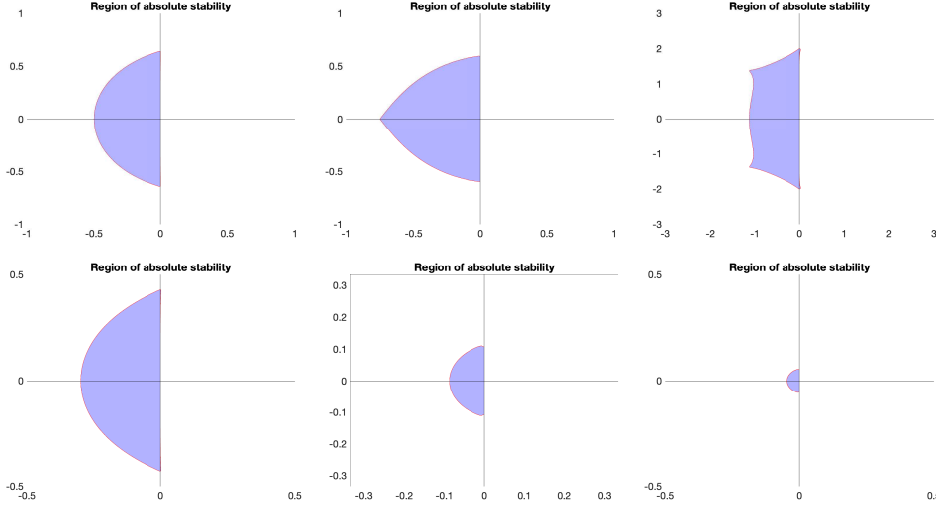


FIG. 1. *Stability regions of the eEIS+(2,4) (left), eEIS+(3,6) (middle), and eEIS+(5,7) (left). Bottom: stability regions of Adams-Bashforth methods of the corresponding orders.*

These methods were constructed to maximize the linear stability region. In Figure 1 we show the stability regions of these methods, and compare them to stability regions of the Adams-Bashforth linear multistep methods with corresponding orders given in [10].

When comparing these regions of stability, we need to keep in mind that while the linear multistep methods require only one function evaluation per time step, the general linear methods have intermediate stages at which the function evaluation is computed, which increases the computational cost to get to the final time. For example, when looking at the eEIS+(2,4) method we need to compute two stages, so that we require two function evaluations at each time-step. For a fair comparison, the stability regions need to be scaled as well: for this reason, in Figure 1 the figure presented is visually scaled by the length of V^n , in that while for the eEIS+(2,4) method we show the axes as $(-1, 1)$, for the fourth order Adams-Bashforth method the axes are $(-0.5, 0.5)$. Similarly, the axes for the eEIS+(3,6) are $(-1, 1)$ while for the corresponding sixth order Adams-Bashforth method the axes are $(-0.33, 0.33)$, and for the eEIS+(5,7) the axes are $(-2.5, 2.5)$ and the corresponding seventh order Adams-Bashforth method has axes $(-0.5, 0.5)$. (Note that for an explicit method, we also may have some elements of $F(V^{n+1})$ to compute at an intermediate stage, but these will be needed anyway at the next time-step so they do not add to the computational cost.)

Explicit error inhibiting method eEIS+(4,4) with lower computational cost: This explicit four stage error inhibiting method is fourth order if it is post processed, otherwise it gives third order accurate solutions. It is interesting because only two values of F are computed, so it has the computational cost of a $s = 2$ method. The coefficients are:

$$\mathbf{D} = \frac{1}{30} \begin{pmatrix} 84 & -47 & -20 & 13 \\ 84 & -47 & -20 & 13 \\ 84 & -47 & -20 & 13 \\ 84 & -47 & -20 & 13 \end{pmatrix}, \quad \mathbf{A} = \frac{1}{240} \begin{pmatrix} 0 & 259 & 0 & 77 \\ 0 & 214 & 0 & 182 \\ 0 & 139 & 0 & 317 \\ 0 & 34 & 0 & 482 \end{pmatrix}.$$

The abscissas are $c_1 = -3/4, c_2 = -1/2, c_3 = -1/4, c_4 = 0$. The truncation error vector is: $\boldsymbol{\tau}_3 = \frac{1}{480} (-29, -69, -154, -299)^T$.

Explicit error inhibiting method eEIS+(3,6): This explicit three stage error inhibiting method is sixth order if it is post processed, otherwise it gives fifth order accurate solutions. The coefficients are:

$$\mathbf{D} = \begin{pmatrix} 0.844429704970785 & 0.183161240819666 & -0.027590945790451 \\ 0.844429704970785 & 0.183161240819666 & -0.027590945790451 \\ 0.844429704970785 & 0.183161240819666 & -0.027590945790451 \end{pmatrix},$$

$$\mathbf{A} = \begin{pmatrix} 0.119782131013886 & 0.530075444729337 & 0.295068834365335 \\ 0.034108245281186 & 0.972302193339061 & -2.090901330553469 \\ -0.067206259640574 & 1.216836100819247 & -0.661223528969050 \end{pmatrix},$$

$$\mathbf{R} = \begin{pmatrix} 0 & 0 & 0 \\ 2.464399360954857 & 0 & 0 \\ 0.210685805002394 & 1.137368201889378 & 0 \end{pmatrix}.$$

The abscissas are $c_1 = -0.891535334604278, c_2 = -0.456552374616537, c_3 = 0$. The truncation error vector is:

$$\boldsymbol{\tau}_5 = (0.002851625181111, -0.041196333074551, -0.186205087415322)^T.$$

Explicit error inhibiting method eEIS(5,7): This explicit three stage error inhibiting method is seventh order if it is post processed, otherwise it gives sixth order accurate solutions. The coefficients are given in the full 5×5 matrices \mathbf{D} , \mathbf{A} , and the strictly lower triangular matrix \mathbf{R} . The coefficients in these matrices are:

$$d_{i1} = -1.011623735666550, \quad d_{i2} = 1.095449867712963, \quad d_{i3} = 1.789431260361622, \\ d_{i4} = -0.872726291980225, \quad d_{i5} = -0.000531100427809, \quad \text{for } i = 1, \dots, 5.$$

$$a_{11} = 0.542403428557849, \quad a_{12} = -0.760948514260222, \quad a_{13} = 0.540150963081669, \\ a_{14} = 0.159072579950024, \quad a_{15} = 0.391433932478452, \\ a_{21} = 0.156488609423175, \quad a_{22} = -0.242186890762633, \quad a_{23} = 0.247855775765120, \\ a_{24} = 0.363064760009647, \quad a_{25} = 0.314695085548473, \\ a_{31} = -0.052321607410313, \quad a_{32} = 0.097345632885763, \quad a_{33} = -0.221816006761698, \\ a_{34} = 0.900744500805372, \quad a_{35} = -0.013037891925596, \\ a_{41} = 0.396379418407651, \quad a_{42} = -0.498665400266501, \quad a_{43} = 0.102234339427055, \\ a_{44} = 0.658422701253808, \quad a_{45} = -0.027557926231150, \\ a_{51} = 1.449809317440111, \quad a_{52} = -1.855043289819523, \quad a_{53} = 0.795025316417296, \\ a_{54} = 0.015237452869142, \quad a_{55} = 0.383077291565467.$$

$r_{21} = .067750736449434$, $r_{31} = -0.970866150021656$, $r_{32} = 1.411026181526863$,
 $r_{41} = 1.110541182884615$, $r_{42} = -0.861259710862469$, $r_{43} = 0.461581912124537$,
 $r_{51} = 0.142695702867824$, $r_{52} = 0.803890471392162$, $r_{53} = -1.532866050532452$,
 $r_{54} = 1.507618973979455$, and $r_{ij} = 0$ whenever $j \geq i$.

The abscissas are $c_1 = -0.837332796371710$, $c_2 = -0.801777109746265$,
 $c_3 = -0.558370527080746$, $c_4 = -0.367768669441936$, with $c_5 = 0$. The truncation
 error vector is:

$$\boldsymbol{\tau}_6 = \begin{bmatrix} -2.452136279362326 \times 10^{-3} \\ -9.952624484663908 \times 10^{-4} \\ -6.583335089187866 \times 10^{-3} \\ -1.186500759891287 \times 10^{-2} \\ -6.616898102859160 \times 10^{-2} \end{bmatrix}$$

Strong stability preserving methods [11] are of interest for the time evolution of
 hyperbolic problems with shocks or sharp gradients. These high order time-stepping
 methods preserve the nonlinear, non-inner-product strong stability properties of the
 spatial discretization coupled with forward Euler time-stepping. The following two
 methods show that it is possible to combine the EIS+ and SSP properties in a given
 method. Although these methods are SSP, the post-processor is not. However, we
 are not worried that the post-processor will destroy the nonlinear stability properties
 because frequently these properties are only important for the stability of the time
 evolution, but not necessarily needed at the final time.

Explicit SSP error inhibiting method eSSP-EIS(3,4) This explicit three step
 error inhibiting method is fourth order if it is post processed, otherwise it gives third
 order accurate solutions. This method is strong stability preserving (SSP) with SSP
 coefficient $C = 0.7478$. The coefficients of this method are:

$$\mathbf{D} = \begin{pmatrix} 0.481236169483274 & 0 & 0.518763830516726 \\ 0.481236169483274 & 0 & 0.518763830516726 \\ 0.481236169483274 & 0 & 0.518763830516726 \end{pmatrix}$$

$$\mathbf{A} = \begin{pmatrix} 0 & 0 & 0.693711877859443 \\ 0.081596114968722 & 0 & 0.333227135691426 \\ 0.167078858485521 & 0 & 0.331269986340461 \end{pmatrix}$$

$$\mathbf{R} = \begin{pmatrix} 0 & 0 & 0 \\ 0.642348436974698 & 0 & 0 \\ 0.254975180593489 & 0.530807045380761 & 0 \end{pmatrix}$$

The abscissas are $c_1 = -0.590419192940789$, $c_2 = -0.226959383165386$, $c_3 = 0$.
 The truncation error vector is

$$\boldsymbol{\tau}_3 = \begin{bmatrix} -5.591881250375826 \\ -5.080104811229902 \\ 5.187361482884723 \end{bmatrix} \times 10^{-2}$$

The SSP coefficient of this method compares favorably to the SSP coefficients of
 linear multistep methods: to obtain a fourth order linear multistep method we need
 five steps and the SSP coefficient is small: $C = 0.021$. Even a linear multistep method

with fifty steps has a smaller SSP coefficient $C = 0.561$. However, a comparison with Runge–Kutta methods is less favorable: the low storage three-stage third order Shu–Osher SSP Runge–Kutta method has SSP coefficient $C = 1$ with the same number of function evaluations and lower storage. Scaled by the number of function evaluations we obtain an effective SSP coefficient of $C/3 \approx 0.33$, whereas our current method has an effective SSP coefficient $C/3 \approx 0.25$. Our method is still competitive here because it is fourth order rather than third. However, if we compare to the five stage fourth order SSP Runge–Kutta method which has SSP coefficient $C = 1.5$, ($C/5 = 0.3$), or to the low storage ten stage fourth order SSP Runge–Kutta method has SSP coefficient $C = 6$ ($C/10 = 0.6$), our method is not as efficient. The more correct comparison is to multi-step Runge–Kutta methods in [2]: the three-stage, three-step fourth order method here has an effective SSP coefficient $C/3 \approx 0.39$, which is higher than the eSSP-EIS(3,4).

Explicit SSP error inhibiting method eSSP-EIS(4,5) This four stage error inhibiting methods is fifth order if it is post processed, otherwise it gives fourth order accurate solutions. This method is strong stability preserving (SSP) with SSP coefficient $C = 0.643897$ (or an effective SSP coefficient $C/4 \approx 0.16$). This method is interesting because all SSP multistep methods require at least seven steps for fifth order and have very small SSP coefficients which make them inefficient. There are no fifth order SSP Runge–Kutta methods [11], however we can compare this method with the SSP multistep multistage methods in [2]: where the corresponding four step four stage method has effective SSP coefficient $C/4 = 0.38436$, which is more efficient.

The coefficients of the eSSP-EIS(4,5) are:

$$\mathbf{D} = \begin{pmatrix} d_1 & d_2 & d_3 & d_4 \\ d_1 & d_2 & d_3 & d_4 \\ d_1 & d_2 & d_3 & d_4 \\ d_1 & d_2 & d_3 & d_4 \end{pmatrix} \quad \text{where} \quad \begin{pmatrix} d_1 \\ d_2 \\ d_3 \\ d_4 \end{pmatrix} = \begin{pmatrix} 0.391361993111787 \\ 0.065690723540339 \\ 0.209839489692975 \\ 0.333107793654898 \end{pmatrix}$$

$$\mathbf{A} = \begin{pmatrix} 0.111982379086567 & 0 & 0 & 0.517330861095791 \\ 0.144956804626331 & 0 & 0 & 0.200688177229557 \\ 0.039506390225419 & 0.074215962133829 & 0.237072128025406 & 0.190419328868168 \\ 0.013111528886920 & 0.067038414113032 & 0.296412681422031 & 0.277723998040954 \end{pmatrix}$$

$$\mathbf{R} = \begin{pmatrix} 0 & 0 & 0 & 0 \\ 0.602472175831079 & 0 & 0 & 0 \\ 0.164197196121254 & 0.423264977696018 & 0 & 0 \\ 0.054494380980164 & 0.140474767505132 & 0.515429866206022 & 0 \end{pmatrix}$$

The abscissas are $c_1 = -0.735372396971898$, $c_2 = -0.416568479467288$, $c_3 = -0.236009654084161$, and $c_4 = 0$. The truncation error vector is

$$\boldsymbol{\tau}_4 = \begin{bmatrix} -1.648864820077294 \\ -4.617774532209270 \\ 0.7007842214544382 \\ 2.406415533885425 \end{bmatrix} \times 10^{-2}$$

4.2. Implicit Methods. In this section we present several implicit error inhibiting methods that can be post-processed. For each method we present the coefficients \mathbf{D} , \mathbf{A} , \mathbf{R} , as well as values of the abscissas and the truncation error vector that must be used to construct the postprocessor. We denote an implicit s -step method that

satisfies the conditions (23) and can be postprocessed to order p as $\text{iEIS}+(s,p)$. All the methods we present are A-stable, so we do not show their stability regions here. **A-stable implicit method $\text{iEIS}+(2,3)$.** This A-stable implicit two stage error inhibiting method is third order if it is post processed, otherwise it gives second order accurate solutions. The coefficients are given in:

$$\mathbf{D} = \begin{pmatrix} 2 & -1 \\ 2 & -1 \end{pmatrix}, \quad \mathbf{A} = \frac{1}{12} \begin{pmatrix} 13 & -14 \\ 16 & -24 \end{pmatrix}, \quad \mathbf{R} = \frac{1}{12} \begin{pmatrix} 19 & 0 \\ 24 & 8 \end{pmatrix}.$$

Here the abscissas are $c_1 = -\frac{1}{2}, c_2 = 0$, and the truncation error vector is $\boldsymbol{\tau}_2 = \left(\frac{3}{8}, \frac{3}{4}\right)^T$.

The cost of the implicit solve is often non-trivial, and the computation can be speeded up if the method admits an efficient parallel implementation. For this reason, we added the requirement in our optimization code that \mathbf{R} is a diagonal matrix. All the following methods are efficient when implemented in parallel.

Parallel-efficient A-stable implicit method $\text{iEIS}+(2,3)$. This two stage error inhibiting method is third order if it is post processed, otherwise it gives second order accurate solutions. This method is A-stable implicit with diagonal \mathbf{R} allowing the implicit solves to be performed concurrently. The coefficients are given in:

$$\mathbf{D} = \frac{1}{15} \begin{pmatrix} 16 & -15 \\ 16 & -15 \end{pmatrix}, \quad \mathbf{A} = \frac{1}{480} \begin{pmatrix} 75 & 106 \\ -1440 & 736 \end{pmatrix}, \quad \mathbf{R} = \frac{1}{32} \begin{pmatrix} 21 & 0 \\ 0 & 96 \end{pmatrix}.$$

Here the abscissas are $c_1 = -\frac{1}{2}, c_2 = 0$, and the truncation error vector is $\boldsymbol{\tau}_2 = \left(\frac{1}{120}, (31, 496)^T\right)$.

Parallel-efficient A-stable implicit method $\text{iEIS}+(3,4)$ This three stage error inhibiting method is fourth order if it is post processed, otherwise it gives third order accurate solutions. This method is A-stable implicit with diagonal \mathbf{R} allowing the implicit solves to be performed concurrently. The coefficients are given in:

$$\mathbf{D} = \begin{pmatrix} 1.100594730800523 & -0.335370831614021 & 0.234776100813498 \\ 1.100594730800523 & -0.335370831614021 & 0.234776100813498 \\ 1.100594730800523 & -0.335370831614021 & 0.234776100813498 \end{pmatrix}$$

$$\mathbf{A} = \begin{pmatrix} 0.806950212712456 & -0.386181733528596 & -0.182046279153154 \\ 2.687898652721551 & -1.944296251569286 & -1.165162710461159 \\ 1.052813949541399 & -0.265689012035030 & -0.052553462549502 \end{pmatrix}$$

$$\mathbf{R} = \begin{pmatrix} 0.716550676631637 & 0 & 0 \\ 0 & 1.710166519304569 & 0 \\ 0 & 0 & 0.887368068372141 \end{pmatrix}$$

Here the abscissas are $c_1 = -\frac{2}{3}, c_2 = -\frac{1}{3}, c_3 = 0$, and the truncation error vector is

$$\boldsymbol{\tau}_3 = (0.278446186799822, 1.535336949555884, 0.887870711092943)^T.$$

Parallel-efficient A-stable implicit method $\text{iEIS}+(4,5)$. This four stage error inhibiting method is fifth order if it is post processed, otherwise it gives fourth order accurate solutions. This method is A-stable implicit with diagonal \mathbf{R} allowing the

implicit solves to be performed concurrently. The coefficients are given in:

$$\mathbf{D} = \begin{pmatrix} d_1 & d_2 & d_3 & d_4 \\ d_1 & d_2 & d_3 & d_4 \\ d_1 & d_2 & d_3 & d_4 \\ d_1 & d_2 & d_3 & d_4 \end{pmatrix} \quad \text{where} \quad \begin{pmatrix} d_1 \\ d_2 \\ d_3 \\ d_4 \end{pmatrix} = \begin{pmatrix} -2.189053680903935 \\ 3.606949225806165 \\ -0.710842571233197 \\ 0.292947026330966 \end{pmatrix}$$

$$\mathbf{R} = \begin{pmatrix} r_1 & 0 & 0 & 0 \\ 0 & r_2 & 0 & 0 \\ 0 & 0 & r_3 & 0 \\ 0 & 0 & 0 & r_4 \end{pmatrix} \quad \text{where} \quad \begin{pmatrix} r_1 \\ r_2 \\ r_3 \\ r_4 \end{pmatrix} = \begin{pmatrix} 0.243205109444297 \\ 0.428641943283907 \\ 1.223508778356526 \\ 0.861606621761651 \end{pmatrix}$$

and:

$$\mathbf{A} = \begin{pmatrix} 0.542633235622690 & 0.572906890966515 & -0.147775065138658 & 0.108270009767368 \\ -0.935354930827541 & 1.187517922840311 & 0.040246733851822 & -0.237077959731666 \\ -3.856502347754360 & 5.000000000000000 & 3.366967278814666 & -5.000000000000000 \\ -3.605680346039871 & 4.951687114045852 & 1.612027197556519 & -2.835666877907317 \end{pmatrix}$$

Here the abscissas are $c_1 = -\frac{3}{4}, c_2 = -\frac{1}{2}, c_3 = -\frac{1}{4}, c_4 = 0$, and the truncation error vector is

$$\boldsymbol{\tau}_4 = \begin{bmatrix} 0.044949370534240 \\ 0.165996341680758 \\ 1.268926100495425 \\ 1.371111036428543 \end{bmatrix}.$$

5. Numerical Results. In this section we test the methods presented in Section 4 on a selection of numerical test cases. Most of the numerical studies are designed to show that the methods achieve the desired convergence rates on nonlinear scalar and systems of ODEs, as well as systems of ODEs resulting from semi-discretizations of PDEs. We also explore the behavior of the SSP methods in terms of preserving the total variation diminishing properties of spatial discretizations, and the issue of order reduction that occurs in implicit methods.

5.1. Comparison of explicit schemes. In Section 4.1 we presented several explicit EIS schemes that can be post-processed to attain higher order. Here we demonstrate that these methods attain the design order of convergence on several standard test cases.

Nonlinear scalar ODE: We compare the performance of several two-step schemes on the nonlinear ODE

$$y' = -y^2$$

with initial condition $y(0) = 2$. The methods we consider here are:

- A non-EIS two step second order method presented by Butcher in [3]

$$V^{n+1} = \frac{1}{4} \begin{pmatrix} -3 & 7 \\ -3 & 7 \end{pmatrix} V^n + \frac{\Delta t}{8} \begin{pmatrix} -3 & -3 \\ -7 & 9 \end{pmatrix} F(V^n)$$

abscissas are $c_1 = 1, c_2 = 2$. (Note that the abscissas are different in John Butcher's formulation).

- An eEIS(2,3) method presented in [6]

$$V^{n+1} = \frac{1}{6} \begin{pmatrix} 7 & -1 \\ 7 & -1 \end{pmatrix} V^n + \frac{\Delta t}{24} \begin{pmatrix} 1 & 125 \\ -17 & 55 \end{pmatrix} F(V^n)$$

abscissas are $c_1 = -\frac{1}{2}, c_2 = 0$.

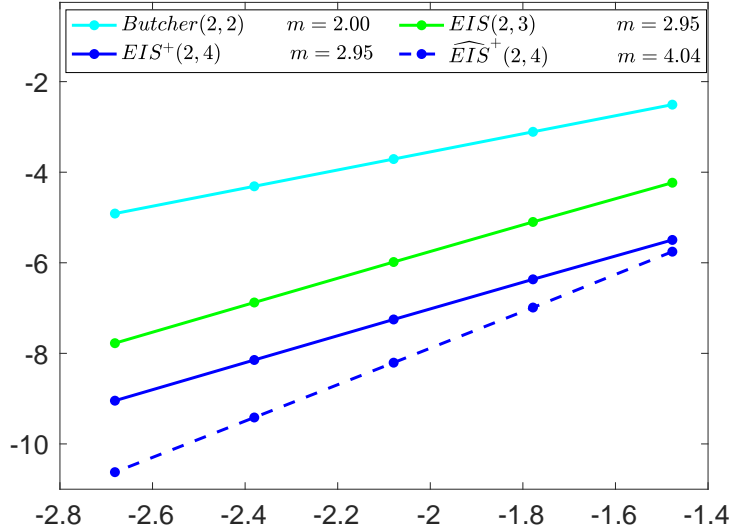


FIG. 2. Convergence of several two-step schemes on a nonlinear scalar test problem. On the x -axis is \log_{10} of time-step and on the y -axis is \log_{10} of the errors. The non-EIS method by Butcher (in cyan solid) shows second order convergence, while the EIS method (in green solid) shows third order. The $eEIS+(2,4)$ method (blue solid) is third order as well, but with a smaller error constant. Finally, when the results of the $eEIS+(2,4)$ method for the final time $T_f = 1$ are postprocessed (blue dashed), fourth order convergence is obtained.

- The $eEIS+(2,4)$ method presented in Section 4.1.

Figure 2 shows the convergence history of each of these methods. The non-EIS method by Butcher (in cyan) shows clear second order, while the EIS method (in green) shows third order. The $eEIS+(2,4)$ method (blue, denoted $EIS+$ in legend) is third order as well, but with a smaller error constant. Finally, when the results of the $eEIS+(2,4)$ method for the final time $T_f = 1.0$ are postprocessed (dashed blue line), fourth order convergence is obtained (denoted $\widehat{EIS}+$ in legend).

Non-stiff Van der Pol oscillator: The nonlinear system of ODEs is given by

$$\begin{pmatrix} y_1 \\ y_2 \end{pmatrix}' = \begin{pmatrix} y_2 \\ (1 - y_1^2)y_2 - y_1 \end{pmatrix}$$

with initial condition $\mathbf{y}(0) = (2, 0)^T$. We use the explicit methods $eEIS+(2,4)$, $eEIS+(3,6)$, $eEIS+(5,7)$ to evolve this problem to the final time $T_f = 2.0$ and post-process the solution at the final time as described in Section 3.3. In Figure 3 we show the errors for different values of Δt for y_1 on the left and y_2 on the right. The slopes of these lines are computed using MATLAB's `polyfit` function and are shown in the legend. This example verifies that numerical solutions from the $eEIS+$ methods attain the expected orders of convergence with and without post-processing.

Advection-diffusion problem: We solve the advection–diffusion problem

$$u_t + au_x = bu_{xx}$$

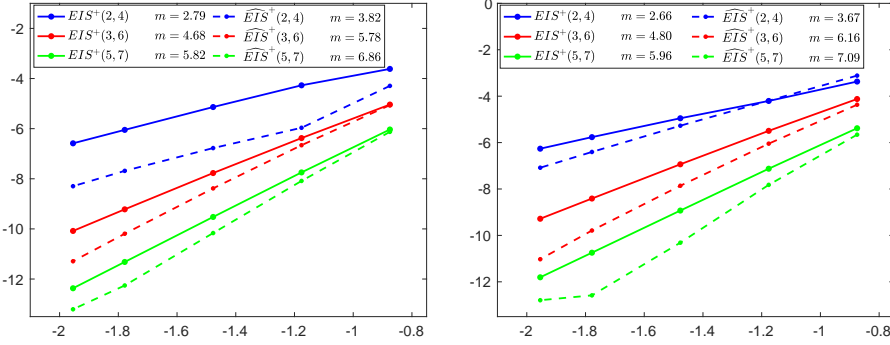


FIG. 3. Convergence of the postprocessed solution from evolving the Van der Pol system to time $T_f = 2.0$ using $eEIS+(2,4)$, $eEIS+(3,6)$, and $eEIS+(5,7)$ methods for the non-stiff Van der Pol system. Left: the \log_{10} errors in the first element, y_1 , for various time-steps. Right: the same for the second element y_2 .

with periodic boundary conditions $u(0, t) = u(2\pi, t)$ and initial condition

$$u(x, 0) = \sin(5x).$$

Here we use $a = 1.0$ and $b = 0.1$. We discretize the problem in space with $N = 41$ points using a Fourier spectral method to obtain the ODE

$$y' = \left(-D_x + \frac{1}{10} D_x^2 \right) y,$$

where D_x is the first order Fourier differentiation matrix and D_x^2 is the second order Fourier differentiation matrix. Due to the periodicity of this problem, the spatial differentiation is exact and so the errors arise only from the time evolution of this ODE.

We evolve this problem forward to final time $T_f = 1.0$ using the $eEIS+(s,p)$ methods presented in Section 4.1 with $\Delta t = T_f/M$, and postprocess the solution at the final time as described in Section 3.3. In Table 1 we show the errors for different values of $M = 1/\Delta t$ before and after postprocessing. We observe that the errors are of the predicted EIS order (which is one order higher than predicted by a truncation error analysis) before post-processing and gain an order after postprocessing, as expected.

Next, we study the SSP properties of the $eSSP-EIS+$ schemes presented in Section 4.1. To do so, we look at a problem where the spatial discretization is total variation diminishing when coupled with forward Euler time-stepping, and examine the maximal rise in total variation when this problem is evolved forward with an $eSSP-EIS+$ scheme.

SSP study: As two of our explicit methods are strong stability preserving, we demonstrate their ability to preserve the total variation diminishing property of a first-order upwind spatial difference applied to Burgers' equation with step function initial conditions:

$$u_t + \left(\frac{1}{2} u^2 \right)_x = 0 \quad u(0, x) = \begin{cases} 1, & \text{if } 0 \leq x \leq 1/2 \\ 0, & \text{if } x > 1/2 \end{cases}$$

method	M	at final time		post-processed	
		error	order	error	order
eEIS+(2,4)	100	6.52×10^{-6}	–	1.01×10^{-6}	–
	150	1.83×10^{-6}	3.13	1.96×10^{-7}	4.04
	200	7.52×10^{-7}	3.09	6.16×10^{-8}	4.03
	250	3.78×10^{-7}	3.07	2.50×10^{-8}	4.02
	300	2.16×10^{-7}	3.06	1.20×10^{-8}	4.02
eEIS+(4,4)	100	1.76×10^{-5}	–	3.28×10^{-6}	–
	150	5.46×10^{-6}	2.89	6.52×10^{-7}	3.98
	200	2.36×10^{-6}	2.92	2.07×10^{-7}	3.99
	250	1.22×10^{-6}	2.94	8.50×10^{-8}	3.99
	300	7.15×10^{-7}	2.95	4.11×10^{-8}	3.99
eEIS+(3,6)	100	1.94×10^{-9}	–	4.90×10^{-10}	–
	150	2.37×10^{-10}	5.18	4.19×10^{-11}	6.06
	200	5.44×10^{-11}	5.12	7.34×10^{-12}	6.05
	250	1.74×10^{-11}	5.09	1.91×10^{-12}	6.02
	300	6.90×10^{-12}	5.08	6.52×10^{-13}	5.90
eEIS+(5,7)	35	3.34×10^{-9}	–	8.27×10^{-10}	–
	40	1.50×10^{-9}	6.00	3.25×10^{-10}	6.97
	45	7.41×10^{-10}	5.99	1.43×10^{-10}	6.98
	50	3.94×10^{-10}	5.99	6.86×10^{-11}	6.98
	55	2.22×10^{-10}	5.99	3.52×10^{-11}	6.99

TABLE 1

Convergence of the solution from evolving the advection-diffusion equation problem to time $T_f = 1$ using different eEIS methods with and without post-processing.

on the domain $[0, 1]$ with periodic boundary conditions. We used a first-order upwind difference to semi-discretize, with 200 spatial points, the nonlinear spatial terms $N(u) \approx -\left(\frac{1}{2}u^2\right)_x$.

We evolve the solution 10 time-steps using the SSP methods eSSP-EIS(3,4) and eSSP-EIS(4,5) for different values of Δt . At each time-level y^n we compute the total variation of the solution at time u^n ,

$$\|u^n\|_{TV} = \sum_j |u_{j+1}^n - u_j^n|.$$

The maximal rise in total variation (solid line with circle markers) is graphed against $\lambda = \frac{\Delta t}{\Delta x}$ in Figure 4. We then post-process the solution at the final time for all values of Δt before the total variation begins to rise, and compute the difference between the total variation of the solution at the final time and the postprocessed solution

$$\|u^n\|_{TV} - \|\hat{u}^n\|_{TV}$$

In the left graph of Figure 4 we see that the eSSP-EIS(3,4) preserves the total variation diminishing property up to $\lambda \approx 1.2$ (larger than the predicted value of $\lambda \leq 0.75$). We compare the maximal rise in total variation from the eSSP-EIS(3,4) method (blue solid line) to the maximal rise in total variation from the eEIS(2,4) method (cyan dashed line), which is not SSP, and indeed we see that the total variation is comparatively large for even small values of Δt . The maximal difference between the total variation of the solution and the post-processed solution (red dashed line) also remains small ($\approx 10^{-14}$).

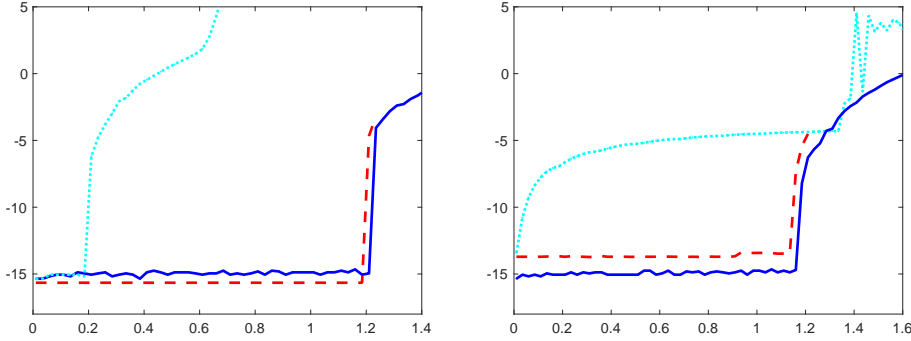


FIG. 4. *SSP study: the eSSP-EIS methods were used to evolve forward the solution in time of Burgers' equation with a step function initial conditions. On the y-axis is \log_{10} of the maximal rise in total variation, and on the x-axis the CFL number λ . The blue solid line is the maximal rise in total variation from the eSSP-EIS method without post-processing. The cyan dotted line is the maximal rise in total variation from the non-SSP method. The red dashed line is the difference between the total variation of the un-processed solution and that of the post-processed solution. Left: eSSP-EIS+(3,4) compared to the eEIS+(2,4) method. Right: eSSP-EIS+(4,5) compared to the implicit eEIS+(4,5) method.*

On the right graph of Figure 4 we see that the eSSP-EIS(4,5) preserves the total variation diminishing property up to $\lambda \approx 1.16$ (larger than the predicted value of $\lambda \leq 0.63$). We compare the eSSP-EIS(4,5) method to the implicit non-SSP iEIS+(4,5) method presented in Section 4.2. Clearly, the maximal rise in total variation of the implicit non-SSP method (dotted cyan line) is large for any Δt , while the maximal rise in total variation from the eSSP-EIS(4,5) method (blue solid line) remains very small ($\approx 10^{-15}$) up to $\lambda \approx 1.16$. The maximal difference between the total variation of the solution and the post-processed solution (red dashed line) also remains small ($\approx 10^{-14}$).

We see that the difference between the total variation of the solution at the final time and the postprocessed solution is minimal for almost all the values of Δt for which the maximal rise in total variation remains bounded. We observe a jump in total variation of the post-processed solution occurs for a slightly smaller Δt than the value at which we observe the jump in the total variation of the un-processed solution u^n . Although the method itself was designed to be SSP, the post-processor is only designed to extract a higher order solution but not to preserve the strong stability properties. This is not a concern because preserving the nonlinear stability properties is generally only important for the stability of the time evolution: once we reach the final time solution these properties are no longer needed. Although we do not expect the post-processor to preserve the nonlinear stability properties that the time-evolution does preserve, it is pleasant to see that for this case it does indeed do so for most relevant values of Δt .

5.2. Comparison of implicit schemes. In Section 4.2 we presented implicit EIS schemes that can be post-processed to attain higher order. Here we demonstrate that these methods attain the design order of convergence on several standard test cases, and show that although these methods suffer from order reduction (as expected from implicit schemes that have lower stage order than overall order) the size of the errors is still small.

M	at final time		post-processed		at final time		post-processed	
	iEIS+(2,3)				iEIS+(2,3) _p			
	error	ord.	error	ord.	error	ord.	error	ord.
16	1.10×10 ⁻⁵	–	8.56×10 ⁻⁶	–	2.81×10 ⁻⁶	–	2.57×10 ⁻⁶	–
32	2.41×10 ⁻⁶	2.19	1.29×10 ⁻⁶	2.72	5.71×10 ⁻⁷	2.29	3.40×10 ⁻⁷	2.92
48	1.03×10 ⁻⁶	2.08	4.25×10 ⁻⁷	2.73	2.28×10 ⁻⁷	2.26	1.02×10 ⁻⁷	2.96
64	5.73×10 ⁻⁷	2.06	1.90×10 ⁻⁷	2.79	1.20×10 ⁻⁷	2.21	4.35×10 ⁻⁸	2.97
80	3.62×10 ⁻⁷	2.05	1.00×10 ⁻⁷	2.84	7.41×10 ⁻⁸	2.18	2.23×10 ⁻⁸	2.98
	iEIS+(3,4) _p				iEIS+(4,5) _p			
9	1.67×10 ⁻⁵	–	1.47×10 ⁻⁵	–	1.69×10 ⁻⁶	–	8.59×10 ⁻⁷	–
18	9.54×10 ⁻⁷	4.13	8.06×10 ⁻⁷	4.19	7.07×10 ⁻⁸	4.58	4.90×10 ⁻⁸	4.12
36	7.22×10 ⁻⁸	3.72	5.17×10 ⁻⁸	3.96	2.79×10 ⁻⁹	4.66	2.00×10 ⁻⁹	4.61
72	6.17×10 ⁻⁹	3.54	3.27×10 ⁻⁹	3.98	1.33×10 ⁻¹⁰	4.39	7.05×10 ⁻¹¹	4.82
90	2.88×10 ⁻⁹	3.41	1.34×10 ⁻⁹	3.99	1.33×10 ⁻¹⁰	4.39	7.05×10 ⁻¹¹	4.82

TABLE 2

Implicit solvers on Advection diffusion problem. The step-size is $\Delta t = 1/M$ where M is given in the table. Four methods from Section 4.1 are tested. The reference solution is computed by MATLAB's ode45 subroutine.

Advection-diffusion problem: We repeat the advection-diffusion problem above and evolve the ODE

$$y' = \left(-D_x + \frac{1}{10} D_x^2 \right) y,$$

where D_x is the first order Fourier differentiation matrix and D_x^2 is the second order Fourier differentiation matrix based on $N = 41$ points in space. We use the implicit methods iEIS+(2,3), iEIS+(2,3)_p, iEIS+(3,4)_p, and iEIS+(4,5)_p to evolve this problem to the final time $T_f = 1.0$ and postprocess the solution at the final time as described in Section 3.3. Note that $\Delta t = \frac{1}{M}$ can be much larger here than when using explicit methods. We compute the reference solution using MATLAB's ode45 subroutine. The numerical tests confirm that we observe the order of accuracy predicated by the EIS theory for the solution and the post-processed solution.

Prothero–Robinson problem: This problem has been used to reveal the error reduction phenomenon that affects implicit methods. We test our implicit methods on the non-autonomous ODE

$$\frac{dy}{dt} = -a(y - \sin(t)) + \cos(t)$$

with initial condition $y^0 = 0$. We use the values $a = 10$ and $a = 1000$, to show the order reduction phenomenon. We run this problem to final time $T_f = 1.0$ using the iEIS+(s,p)_p methods. Note that this problem has the solution $y = \sin(t)$ regardless of the value of a , making the comparison easy.

Figure 5 (left) shows that the order of convergence for the case $a = 10$ is close to the $p + 1$ design order without post-processing and the enhanced $p + 2$ with post-processing. In contrast, the right graph shows that when $a = 1000$ the convergence rate without post-processing is just what is expected from a truncation error analysis, while after post-processing there is improvement, but the order reduction is still apparent. However, it is important to note that the magnitude of the errors is *smaller* in the case $a = 1000$ than when $a = 10$. In this case, we observe that the order reduction phenomenon is apparent but does not result in an increase of the errors.

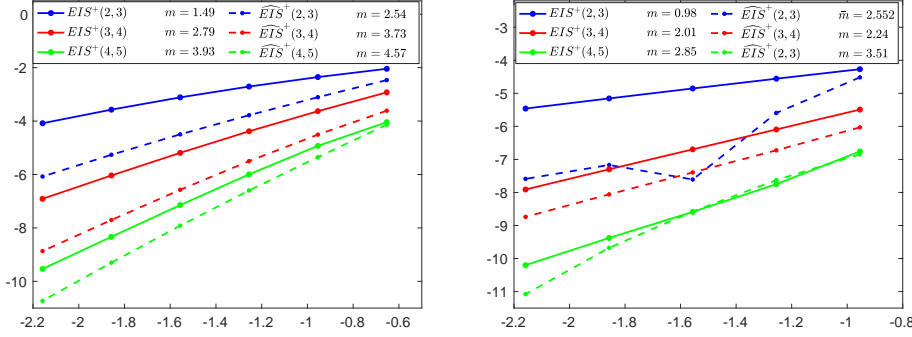


FIG. 5. Convergence test on the Prothero Robinson problem. The x-axis has \log_{10} of the time-step while the y-axis has \log_{10} of the errors. On the left is $a = 10$ and on the right $a = 1000$.

Post-processing in both space and time: The EIS time-stepping approach was motivated by Ditkowski's work [7] on finite difference spatial discretizations for the heat equation whose convergence rates are higher than expected from the order of the truncation error. In this example, we combine the two types of EIS methods (in space and in time) for solving the heat equation. We consider the problem

$$u_t = u_{xx} \quad x \in [0, 1]$$

with periodic boundary conditions and initial conditions

$$u(x, 0) = \cos(2\pi x).$$

Using $N = 41$ points in space we discretize the spatial derivative using the two-point block-type fifth order discretization discussed in [7]:

$$\begin{aligned} \frac{d^2}{dx^2} u_j &= \frac{1}{12(h/2)^2} \left[(-u_{j-1} + 16u_{j-1/2} - 30u_j + 16u_{j+1/2} - u_{j+1}) \right. \\ &\quad \left. - \frac{4}{13} (u_{j-1} - 5u_{j-1/2} + 10u_j - 10u_{j+1/2} + 5u_{j+1} - u_{j+3/2}) \right] \\ \frac{d^2}{dx^2} u_{j+1/2} &= \frac{1}{12(h/2)^2} \left[(-u_{j-1/2} + 16u_j - 30u_{j+1/2} + 16u_{j+1} - u_{j+3/2}) \right. \\ &\quad \left. + \frac{4}{13} (u_{j-1} - 5u_{j-1/2} + 10u_j - 10u_{j+1/2} + 5u_{j+1} - u_{j+3/2}) \right]. \end{aligned}$$

The final time solution can be post-processed in space to obtain sixth order accuracy by taking the FFT of the solution at the final time and then using a hard cut-off filter and transforming back to physical space.

We used the $iEIS+(2,3)_p$ and the $iEIS+(4,5)_p$ methods in time to evolve the solution to final time $T_f = 0.5$ with $\Delta t = \frac{T_f}{256}$. In Figure 6 on the left we show the results from $iEIS+(2,3)_p$. The errors is as the absolute values of the exact and the numerical solutions. The error at the final time is shown in blue (solid line). This error does not improve when postprocessed in space (red stars), probably because the dominant error is coming from the time discretization. When the error is posprocessed

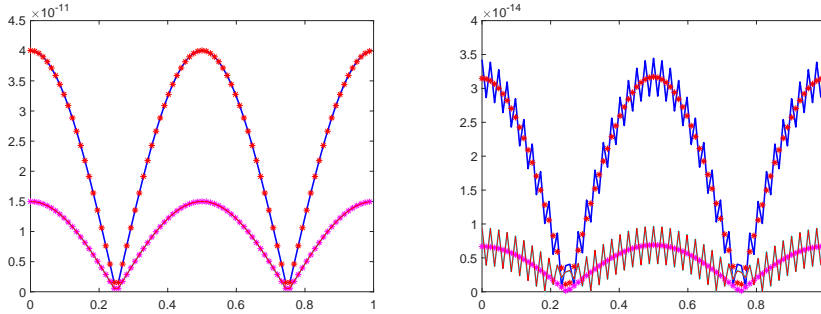


FIG. 6. Block finite difference method with post-processing in space and time. Left: $iEIS+(2,3)_p$. Right: $iEIS+(4,5)_p$. The error is the blue line. Post-processing in space we obtain the red stars. Post-processing in time gives the cyan line. Post-processing in both space and time gives the magenta stars.

in time (cyan line) it becomes much smaller, and post-processing in both time and space (magenta stars) gives essentially the same result. In Figure 6 on the right we show the results from $iEIS+(4,5)_p$. The error at the final time is shown in blue, we notice that it is very oscillatory. This error does get smoother when postprocessed in space (red stars), but the magnitude of the error does not improve. When the error is postprocessed in time (cyan line) it becomes much smaller but is still oscillatory. Finally, post-processing in both time and space (magenta stars) gives a small error that is smooth.

6. Conclusions. In this work we extended the EIS framework in [6] to explicit methods that use function evaluations of newly computed values and to implicit methods. More significantly, we presented additional conditions on the coefficients of the method that allow the final solution to be post-processed in order to extract higher order accuracy. The new EIS conditions (23) not only control the growth of the errors (as we showed in [6]) but also allow us to precisely define the leading error term. Knowing the form of the leading error term we can compute the post-processor defined in 3.3, and apply it to the solution to extract a solution that is two orders of accuracy higher.

We used the new EIS+ framework to formulate an optimization code in MATLAB to find methods that satisfy the order and the EIS+ conditions. We presented some of these EIS+ methods and their stability regions and we tested them on sample problems to show their convergence properties. We confirmed that the numerical solutions coming from these methods are indeed one order higher than expected from a truncation error analysis, and two orders higher when post-processed. In future work, we plan to consider other conditions on \mathbf{D} , \mathbf{A} , \mathbf{R} that allow the error inhibiting behavior to occur, to extend this approach to multi-derivative and implicit-explicit methods, and to create variable step-size methods with EIS properties

Appendix A. An alternative error analysis.

In this section we provide an alternative proof for the accuracy of the proposed schemes. This proof is similar to the one given in [6]. This proof directly tracks the dynamics of the error, rather than tracking the behavior of the solution, as we did in Section 3.2.

We write the scheme as

$$(35) \quad (I - \Delta t \mathbf{R}F) V^{n+1} = (\mathbf{D} + \Delta t \mathbf{A}F) V^n,$$

where we assume, as we did above, that the scheme (4) (equivalently (35)) is zero-stable, so that the operator $(I - \Delta t \mathbf{R}F)^{-1}$ is bounded. In order to evaluate the operator $(I - \Delta t \mathbf{R}F)$ we use Lemma 2 to obtain:

$$(36) \quad \begin{aligned} F(V^{n+1}) &= F(U^{n+1} + E^{n+1}) \\ &= F(U^{n+1}) + F_y^{n+1} E^{n+1} + O(\Delta t) O(\|E^{n+1}\|) + O(\|E^{n+1}\|^2) \\ &= F(U^n) + F_y^n E^{n+1} + O(\Delta t) O(\|E^{n+1}\|), \end{aligned}$$

where, $F_y^n = F_y(u(t_n))$ and $F_y^{n+1} = F_y(u(t_{n+1}))$.

We now subtract (9) from (35), and use (36) to obtain an equation for the relationship between the errors at two successive time-steps:

$$(37) \quad (I - \Delta t \mathbf{R}F_y^n + O(\Delta t^2)) E^{n+1} = (\mathbf{D} + \Delta t \mathbf{A}F_y^n + O(\Delta t^2)) E^n + \tau^{n+1}.$$

For the accuracy analysis we assume that $|F_y^n| = O(1)$, and therefore $\|\Delta t \mathbf{R}F_y^n\| = O(\Delta t) \ll 1$. This observation is then used for approximating

$$(38) \quad (I - \Delta t \mathbf{R}F + O(\Delta t^2))^{-1} = I + \Delta t \mathbf{R}F_y^n + O(\Delta t^2).$$

We then plug this into (37) to obtain a linear recursion relation for the error:

$$(39) \quad \begin{aligned} E^{n+1} &= (I - \Delta t \mathbf{R}F_y^n + O(\Delta t^2))^{-1} [(\mathbf{D} + \Delta t \mathbf{A}F_y^n + O(\Delta t^2)) E^n + \tau^{n+1}], \\ &= (\mathbf{D} + \Delta t F_y^n (\mathbf{R} \mathbf{D} + \mathbf{A}) + O(\Delta t^2)) E^n + (I + \Delta t F_y^n \mathbf{R} + O(\Delta t^2)) \tau^{n+1} \\ &\equiv \hat{Q}^n E^n + \Delta t T_e^n, \end{aligned}$$

where

$$(40) \quad T_e^n = \Delta t^p \tau_{p+1}^{n+1} + \Delta t^{p+1} (\tau_{p+2}^{n+1} + F_y^n \mathbf{R} \tau_{p+1}^{n+1}) + O(\Delta t^{p+2})$$

LEMMA 3. *The equation which governs the dynamics of E^n , (39), is essentially linear in the sense that there is a time interval, $0 \leq t \leq T$, such that the nonlinear terms are of higher order, and thus much smaller, than the leading terms in the equation.*

Proof. It is assumed that the initial numerical condition, V^0 , which is derived by the initial condition of the ODE and other schemes, is either accurate to machine precision or, at least accurate as desired. Thus, at $n = 0$, the scheme is essentially linear.

By assumption, the scheme is zero-stable, therefore

$$\|(\mathbf{D} + \Delta t F_y^n (\mathbf{R} \mathbf{D} + \mathbf{A}) + O(\Delta t^2))\| \leq 1 + c \Delta t \leq \exp(c \Delta t)$$

and, due to the boundedness of F_y^n and \mathbf{R}

$$\|(I + \Delta t F_y^n \mathbf{R} + O(\Delta t^2))\| \leq 2.$$

Therefore,

$$\|E^n\| \leq 2 \frac{\exp(c t_n) - 1}{c \Delta t} \max_{0 \leq \nu \leq n} \|\tau^\nu\|.$$

□

This estimate holds as long as $\|E^n\|^2 \ll O(\Delta t^2) \max_{0 \leq \nu \leq n} \|\tau^\nu\|$.

As the error equation satisfies an iterative process of the form (39), we state the following Lemma that we will use later to understand the dynamics of the growth in the error.

LEMMA 4. *Given an iterative process of the form*

$$(41) \quad W^{n+1} = Q^n W^n + \Delta t F(W^n, t_n)$$

where Q^n is a linear operator, the Discrete Duhamel principle states that

$$(42) \quad W^n = \prod_{\mu=0}^{n-1} Q^\mu W^0 + \Delta t \sum_{\nu=0}^{n-1} \left(\prod_{\mu=\nu+1}^{n-1} Q^\mu \right) F(W^\nu, t_\nu).$$

This is Lemma 5.1.1 in [9] and the proof is given there.

Using the observation that Equation (39), which governs the dynamics of E^n , is essentially linear, we can use the Discrete Duhamel principle, (42) to calculate E^n .

$$(43) \quad E^n = \prod_{\mu=0}^{n-1} \hat{Q}^\mu E_0 + \Delta t \sum_{\nu=0}^{n-1} \left(\prod_{\mu=\nu+1}^{n-1} \hat{Q}^\mu \right) T_e^\nu.$$

The first term in (43) is negligible because we assume that the initial error can be made arbitrarily small. In order to evaluate the second term we divide the sum into three parts:

1. The final term, $\nu = n - 1$, is $\Delta t T_e^{n-1}$ which is clearly of order $\Delta t \|T_e^{n-1}\| = \|\tau^{n+1}\| = O(\Delta t^{p+1})$. This term is the one filtered in the postprocessing stage.
2. The next term, $\nu = n - 2$, is $\Delta t \hat{Q}^{n-1} T_e^{n-2}$. This term can be made of order $\Delta t^2 \|T_e^{n-2}\|$ provided that $\|\hat{Q}^{n-1} T_e^{n-2}\| = O(\Delta t) O(\|T_e^{n-2}\|)$ which is true due to (23a): $\mathbf{D}\tau_{p+1} = 0$.
3. The rest of the sum;

$$(44) \quad \begin{aligned} \left\| \Delta t \sum_{\nu=0}^{n-3} \left(\prod_{\mu=\nu+1}^{n-1} \hat{Q}^\mu \right) T_e^\nu \right\| &= \left\| \Delta t \sum_{\nu=0}^{n-3} \left(\prod_{\mu=\nu+3}^{n-1} \hat{Q}^\mu \right) \left(\hat{Q}^{\nu+2} \hat{Q}_{\nu+1} T_e^\nu \right) \right\| \\ &\leq \Delta t \sum_{\nu=0}^{n-3} \left\| \prod_{\mu=\nu+3}^{n-1} \hat{Q}^\mu \right\| \left\| \hat{Q}^{\nu+2} \hat{Q}_{\nu+1} T_e^\nu \right\| \\ &\leq \Delta t \sum_{\nu=0}^{n-3} (1 + c \Delta t)^{n-\nu-3} \left\| \hat{Q}^{\nu+2} \hat{Q}_{\nu+1} T_e^\nu \right\| \\ &= \frac{\exp(ct_n) - 1}{c} \max_{\nu=0, \dots, n-3} \left\| \hat{Q}^{\nu+2} \hat{Q}_{\nu+1} T_e^\nu \right\|. \end{aligned}$$

Using the definition of the operators \hat{Q}^μ we have:

$$\hat{Q}^{\nu+2} \hat{Q}^{\nu+1} = [\mathbf{D}^2 + \Delta t (F_y^{\nu+2} (\mathbf{RD} + \mathbf{A}) \mathbf{D} + F_y^{\nu+1} \mathbf{D} (\mathbf{RD} + \mathbf{A})) + O(\Delta t^2)]$$

so that $\hat{Q}^{\nu+2}\hat{Q}^{\nu+1}T_e^\nu$ becomes

$$\begin{aligned}
& [\mathbf{D}^2 + \Delta t (F_y^{\nu+2} (\mathbf{R}\mathbf{D} + \mathbf{A}) \mathbf{D} + F_y^{\nu+1} \mathbf{D} (\mathbf{R}\mathbf{D} + \mathbf{A})) + O(\Delta t^2)] T_e^\nu \\
&= \mathbf{D}^2 T_e^\nu + \Delta t F_y^{\nu+2} (\mathbf{R}\mathbf{D} + \mathbf{A}) \mathbf{D} T_e^\nu + F_y^{\nu+1} \mathbf{D} (\mathbf{R}\mathbf{D} + \mathbf{A}) T_e^\nu + O(\Delta t^2) T_e^\nu \\
&= \Delta t^p \mathbf{D}^2 \boldsymbol{\tau}_{p+1}^{\nu+1} + \Delta t^{p+1} \mathbf{D}^2 (\boldsymbol{\tau}_{p+2}^{\nu+1} + F_y^{\nu+1} \mathbf{R} \boldsymbol{\tau}_{p+1}^{\nu+1}) \\
&+ \Delta t^{p+1} F_y^{\nu+2} (\mathbf{R}\mathbf{D} + \mathbf{A}) \mathbf{D} \boldsymbol{\tau}_{p+1}^{\nu+1} + \Delta t^{p+1} F_y^{\nu+1} \mathbf{D} (\mathbf{R}\mathbf{D} + \mathbf{A}) \boldsymbol{\tau}_{p+1}^{\nu+1} + O(\Delta t^{p+2}) \\
&= \Delta t^p (\mathbf{D} + \Delta t F_y^{\nu+2} (\mathbf{R}\mathbf{D} + \mathbf{A}) + \Delta t F_y^{\nu+1} \mathbf{D}\mathbf{R}) \mathbf{D} \boldsymbol{\tau}_{p+1}^{\nu+1} \\
&+ \Delta t^{p+1} \mathbf{D}^2 (\boldsymbol{\tau}_{p+2}^{\nu+1} + F_y^{\nu+1} \mathbf{R} \boldsymbol{\tau}_{p+1}^{\nu+1}) + \Delta t^{p+1} F_y^{\nu+1} \mathbf{D}\mathbf{A} \boldsymbol{\tau}_{p+1}^{\nu+1} + O(\Delta t^{p+2}) \\
&= \Delta t^p (\mathbf{D} + \Delta t F_y^{\nu+2} (\mathbf{R}\mathbf{D} + \mathbf{A}) + \Delta t F_y^{\nu+1} \mathbf{D}\mathbf{R}) \mathbf{D} \boldsymbol{\tau}_{p+1}^{\nu+1} \\
&+ \Delta t^{p+1} (F_y^{\nu+1} \mathbf{D}^2 \mathbf{R} + F_y^{\nu+1} \mathbf{D}\mathbf{A}) \boldsymbol{\tau}_{p+1}^{\nu+1} + \Delta t^{p+1} \mathbf{D}^2 \boldsymbol{\tau}_{p+2}^{\nu+1} + O(\Delta t^{p+2}).
\end{aligned}$$

Using the fact that in our case $\mathbf{D}^2 = \mathbf{D}$ and that $F_y^{\nu+1} = F_y^\nu + O(\Delta t)$ we obtain

$$\begin{aligned}
\hat{Q}^{\nu+2}\hat{Q}^{\nu+1}T_e^\nu &= \Delta t^p (\mathbf{D} + \Delta t F_y^{\nu+2} (\mathbf{R}\mathbf{D} + \mathbf{A}) + \Delta t F_y^{\nu+1} \mathbf{D}\mathbf{R}) \mathbf{D} \boldsymbol{\tau}_{p+1}^{\nu+1} \\
&+ \Delta t^{p+1} F_y^{\nu+1} \mathbf{D} (\mathbf{R} + \mathbf{A}) \boldsymbol{\tau}_{p+1}^{\nu+1} + \Delta t^{p+1} \mathbf{D} \boldsymbol{\tau}_{p+2}^{\nu+1} + O(\Delta t^{p+2}).
\end{aligned}$$

The first term and third terms disappear because of (23a) and (23b)

$$\mathbf{D} \boldsymbol{\tau}_{p+1} = 0 \quad \text{and} \quad \mathbf{D} \boldsymbol{\tau}_{p+2} = 0.$$

The second term is eliminated by (23c)

$$\mathbf{D} (\mathbf{R} + \mathbf{A}) \boldsymbol{\tau}_{p+1} = 0.$$

So that

$$\hat{Q}^{\nu+2}\hat{Q}^{\nu+1}T_e^\nu = O(\Delta t^{p+2}) = O(\Delta t^2)O(\|T_e^\nu\|).$$

Putting this all back together we see that

$$E^n = \Delta t T_e^{n-1} + O(\Delta t^2)O(\|T_e^{n-2}\|) + O(\Delta t^2)O(\|T_e^n\|).$$

Acknowledgment. This publication is based on work supported by AFOSR grant FA9550-18-1-0383 and ONR-DURIP Grant N00014-18-1-2255. A part of this research is sponsored by the Office of Advanced Scientific Computing Research; US Department of Energy, and was performed at the Oak Ridge National Laboratory, which is managed by UT-Battelle, LLC under Contract no. De-AC05-00OR22725. This manuscript has been authored by UT-Battelle, LLC, under contract DE-AC05-00OR22725 with the US Department of Energy. The United States Government retains and the publisher, by accepting the article for publication, acknowledges that the United States Government retains a non-exclusive, paid-up, irrevocable, world-wide license to publish or reproduce the published form of this manuscript, or allow others to do so, for United States Government purposes.

REFERENCES

- [1] M. B. Allen and E. L. Isaacson, *Numerical analysis for applied science*, John Wiley & Sons, 1998.
- [2] C. Breiten, S. Gottlieb, Z. Grant, D. Higgs, D.I. Ketcheson, and A. Nemeth, *Explicit strong stability preserving multistep Runge-Kutta methods*, *Mathematics of Computation* **86** (2017) 747–769.
- [3] J. C. Butcher, *Diagonally-implicit multi-stage integration method*, *Applied Numerical Mathematics* **11** (1993), 347–363.
- [4] J. C. Butcher, *Numerical methods for ordinary differential equations*, John Wiley & Sons, 2008.
- [5] A. Ditkowski, *High order finite difference schemes for the heat equation whose convergence rates are higher than their truncation errors*, *Spectral and High Order Methods for Partial Differential Equations ICOSAHOM 2014*, Springer, 2015, pp. 167–178.
- [6] A. Ditkowski and S. Gottlieb, *Error Inhibiting Block One-step Schemes for Ordinary Differential Equations*, *Journal of Scientific Computing* **73(2)** (2017) 691–711.
- [7] A. Ditkowski *Error inhibiting schemes for differential equations*, lecture given at ICERM on August 2018, https://icerm.brown.edu/video_archive/?play=1669.
- [8] S. Gottlieb, Z.J. Grant, A. Ditkowski, *Explicit and Implicit EIS methods with post-processing*, (2019), GitHub repository, <https://github.com/EISmethods/EISpostprocessing>.
- [9] B. Gustafsson, H.-O. Kreiss, and J. Oliger, *Time dependent problems and difference methods*, vol. 24, John Wiley & Sons, 1995.
- [10] E. Hairer, G. Wanner, and S. P. Norsett, *Solving Ordinary Differential Equations I: Nonstiff Problems*, Springer Series in Computational Mathematics, Springer-Verlag Berlin Heidelberg (1993).
- [11] J. S. Hesthaven, S. Gottlieb, D. Gottlieb, *Spectral Methods for Time Dependent Problems. Cambridge Monographs on Applied and Computational Mathematics (No. 21)*, Cambridge University Press (2006).
- [12] E. Isaacson and H. Keller, *Analysis of numerical methods*, Dover Publications, Inc, 1994.
- [13] Z. Jackiewicz, *General linear methods for ordinary differential equations*, John Wiley & Sons, 2009.
- [14] G.Yu. Kulikov, *On quasi-consistent integration by Nordsieck methods*, *Journal of Computational and Applied Mathematics* **225** (2009) 268–287.
- [15] G. Yu. Kulikov and R. Weiner, *Variable-Stepsize Interpolating Explicit Parallel Peer Methods with Inherent Global Error Control*, *SIAM Journal on Scientific Computing*, **32(4)** (2010) 1695–1723.
- [16] G.Yu. Kulikov and R. Weiner, *Doubly quasi-consistent fixed-stepsize numerical integration of stiff ordinary differential equations with implicit two-step peer methods*, *Journal of Computational and Applied Mathematics*, **340** (2018) 256–275.
- [17] P. D. Lax and R. D. Richtmyer, *Survey of the stability of linear finite difference equations*, *Communications on pure and applied mathematics* **9** (1956), no. 2, 267–293.
- [18] A. Quarteroni, R. Sacco, and F. Saleri, *Numerical mathematics*, vol. 37, Springer Science & Business Media, 2010.
- [19] R.D. Skeel, *Analysis of fixed-stepsize methods*, *SIAM Journal on Numerical Analysis* **13** (1976) 664–685.
- [20] G. Sewell, *The numerical solution of ordinary and partial differential equations*, World Scientific, 2015.
- [21] B. Soleimani, R. Weiner *A class of implicit peer methods for stiff systems*, *Journal of Computational and Applied Mathematics* **316** (2017) 358–368
- [22] R. Weiner, G.Yu. Kulikov, and H. Podhaiskya, *Variable-stepsize doubly quasi-consistent parallel explicit peer methods with global error control*, *Applied Numerical Mathematics* **62** (2012) 1591–1603.
- [23] R. Weiner, B. A. Schmitt, H.Podhaiskya, and S. Jebensc, *Superconvergent explicit two-step peer methods*, *Journal of Computational and Applied Mathematics* **223** (2009) 753–764.